International Journal of Power Electronics and Drive System (IJPEDS)
Vol. 15, No. 4, December 2024, pp. 2145∼2154
ISSN: 2088-8694, DOI: 10.11591/ijpeds.v15.i4.pp2145-2154

Discrete-time Luenberger observer design for Lithium-ion battery state-of-charge with stability guarantee

Harry Septanto[1], Edi Kurniawan[2], Jalu Ahmad Prakosa[2], Samsul Hafiz[1], Made Widhi Surya Atman[3], Oetomo Sudjana[4]
[1]Research Organization for Electronics and Informatics, National Research and Innovation Agency, Bandung, Indonesia
[2]Research Organization for Nanotechnology and Materials, National Research and Innovation Agency, Tangerang Selatan, Indonesia
[3]Faculty of Engineering and Natural Sciences, Tampere University, Tampere, Finland
[4]PT. Teknologi Rakyat Indonesia, Bandung, Indonesia

Article Info

Article history:

Received Mar 4, 2024
Revised Mar 22, 2024
Accepted Mar 28, 2024

Keywords:

Discrete-time
Lithium-ion
Observer
Stability
State-of-charge

ABSTRACT

State-of-charge (SOC) estimation is particularly important as it provides information about the remaining energy capacity of the battery, allowing for better planning and utilization. Accurate SOC estimation is challenging because it cannot be directly measured from the battery. Instead, it is estimated by analyzing measurable variables such as current and voltage. To address this challenge, a discrete-time observer-based SOC estimation approach is proposed in this paper. This approach utilizes a second-order equivalent circuit model and a piecewise linear approximation to represent the relationship between SOC and open circuit voltage (OCV). The proposed observer-based approach utilizes these models to estimate the SOC with assured asymptotic stability under specific assumptions to simplify the design process. Simulations in Python are conducted to evaluate the performance of the designed observer. In the simulations, the SOC estimation under various conditions, such as model uncertainty, disturbances, and measurement noise, is also covered. In addition, three different observer gains are considered in the simulations. Lastly, simulation studies indicate that the estimated SOC values converge to the real SOC values, with some different behavior depending on the regarded situations.

Corresponding Author:

Harry Septanto
Research Organization for Electronics and Informatics, National Research and Innovation Agency
Bandung, Indonesia
Email: harry.septanto@brin.go.id

1. INTRODUCTION

In recent years, the development of electrical vehicles (EVs) has been rapidly growing, which has led to the widespread utilization of batteries as energy storage devices. As technology continues to advance, the demand for higher energy density and faster charging capabilities in lithium-ion batteries (LIBs) has become increasingly vital for the widespread adoption of electric vehicles. LIBs are recognized as the most preferred alternative for EVs due to their numerous benefits, including their high energy storage capacity and long lifespan. [1]-[4]. When using LIBs, monitoring and regulating the charge and discharge operation is crucial since the batteries must be ensured to function as intended, e.g., prevent overcharging and overdischarge, and have a long lifespan [5]-[7]. The LIBs are then complemented with an electronics module known as a battery management system (BMS) to manage these tasks [8]-[12].

The battery monitoring and regulation function in the BMS involves an important variable called state-of-charge (SOC) [3], [13]-[15]. However, this variable cannot measured directly by a sensor. Instead, the SOC must be estimated through measurable variables, i.e., current and (terminal) voltage–the electrical potential difference between two battery polarities. An algorithm for estimating the SOC employs a mathematical model of the battery that accommodates a nonlinear dynamic behavior [16]. A popular model used for it is the equivalent circuit model (ECM). ECM is an electrical circuit dynamic model as an analog to the nonlinear dynamic behavior of a battery [17]. In addition, it models several essential properties of the battery, including internal resistance, resistive-capacitive (RC) time constant, open-circuit voltage (OCV)–the battery's electrical potential difference between two polarities that are disconnected from any load–and nominal capacity [18], [19]. Additionally, ECM is so popular for SOC estimation in BMSs because it meets the computational capacity constraints of BMSs [20].

Many SOC estimation algorithms have been proposed in [21], [22]. However, many of them lack stability guarantees as well as exact rules for determining tuning gains. Therefore, in this study, we propose an observer design based on one first proposed by Luenberger [23] for LIBs SOC estimation with a guarantee of stability from a control theory perspective. In addition, we present some numerical simulations involving the appearance of model uncertainties and disturbances that exist in real-world applications. The preliminary work of this study has been presented and published in [24].

The rest of the paper is organized as follows. Section 2 discusses the battery model, covering the ECM description and the nonlinearity relationship between OCV and SOC. The main results, comprising the observer, stability analysis, numerical simulations, and discussion, are presented in section 3. Lastly, we summarize our study in section 4.

2. METHOD

2.1. Equivalent circuit model

In this study, we use an equivalent circuit model (ECM) with two RCs. This model is well-known as a 2-RC ECM or second-order ECM. Figure 1 illustrates this model. The ordinary differential equation of the 2-RC ECM is presented in (1), (2), (3), and (4), where time $t \geq 0$ and $\dot{V}_1$, as an instance, denotes the first time-derivative of V_1.

$$\dot{V}_1(t) = -\frac{1}{R_1C_1}V_1(t) + \frac{1}{C_1}I(t) \tag{1}$$

$$\dot{V}_2(t) = -\frac{1}{R_2C_2}V_2(t) + \frac{1}{C_2}I(t) \tag{2}$$

$$V_T(t) = V_{OC}(\xi(t)) - R_SI(t) - V_1(t) - V_2(t) \tag{3}$$

Where $V_{OC}(\xi(t))$, or simply V_{OC}, is a nonlinear function representing the relationship between OCV and SOC. While the dynamic equation of the SOC is represented in (4), where Q_ξ is the battery capacity $[Ah]$ and η is Coulombic efficiency–it describes how efficiently a battery transfers electrons during charging and discharging. This form is well-known as a continuous-time version of Coulomb counting.

$$\dot{\xi}(t) = \frac{\eta}{3600 \cdot Q_\xi}I(t) \tag{4}$$

The other parameters and variables of the 2-RC ECM are explained as follows:

- I denotes the battery current $[A]$. It has positive polarity when charging and negative polarity when discharging.
- V_T denotes the terminal voltage $[V]$. It represents the real voltage available for utilization from the battery. The terminal voltage is measured across the terminals when a load is attached to the battery.
- (R_1, C_1) and (R_2, C_2) represent the first and second RC models of the 2-RC ECM, respectively. These relate to the diffusion dynamics [25].
- R_S is also internal resistance $[\Omega]$ of the the 2-RC ECM.

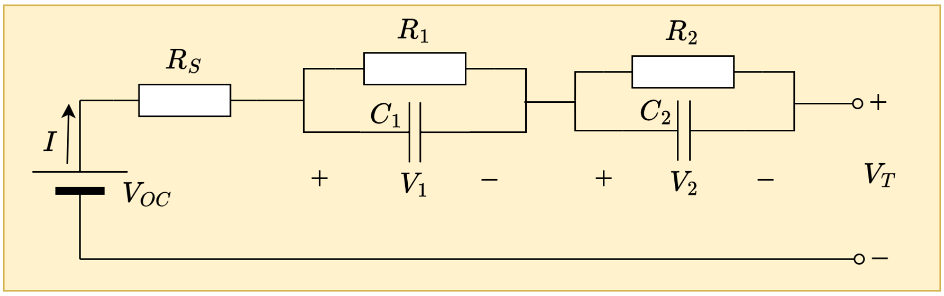

Figure 1. 2-RC equivalent circuit model

Furthermore, an equivalent 2-RC ECM model can be expressed in (5) and (6). This model has a state variable $x(t)$ and an output $y(t)$ which is nonlinear. Note that $(x(t))$ consists of $V_{OC}(\xi(t))$, which is generally a nonlinear function. It will be elaborated on in the following subsection.

$$\begin{cases} \dot{x}(t) = \mathsf{A}x(t) + \mathsf{B}u(t), \\ y(t) = \mathsf{C}(x(t)) + \mathsf{D}u(t) \end{cases} \tag{5}$$

Where

$$\begin{cases} x(t) = \begin{bmatrix} V_1(t) \\ V_2(t) \\ \xi(t) \end{bmatrix}, \\ y(t) = V_T(t), \\ u(t) = I(t), \\ \mathsf{A} = \begin{bmatrix} -\frac{1}{R_1C_1} & 0 & 0 \\ 0 & -\frac{1}{R_2C_2} & 0 \\ 0 & 0 & 0 \end{bmatrix}, \ \mathsf{B} = \begin{bmatrix} \frac{1}{C_1} \\ \frac{1}{C_2} \\ \frac{\eta}{3600 \cdot Q_\xi} \end{bmatrix}, \\ \mathsf{C}(x(t)) = V_{OC}(\xi(t)) - V_1(t) - V_2(t), \ \mathsf{D} = -R_s \end{cases} \tag{6}$$

A discrete-time version of the 2-RC ECM can be realized using Euler's discretization, as indicated in (7) and (8) with the same model parameters A, B, and D as in (6), where $h > 0$ is sampling period $[s]$ and $k = 0, 1, 2, ...$ is the sample sequence.

$$\begin{cases} x(k+1) = (\mathsf{I} + h\mathsf{A})x(k) + h\mathsf{B}u(k) \\ y(k) = \mathsf{C}(x(k)) + \mathsf{D}u(k) \end{cases} \tag{7}$$

Where

$$\begin{cases} x(k) = \begin{bmatrix} V_1(k) \\ V_2(k) \\ \xi(k) \end{bmatrix}, \\ y(k) = V_T(k), \\ u(k) = I(k), \\ \mathsf{C}(x(k)) = V_{OC}(\xi(k)) - V_1(k) - V_2(k), \\ \mathsf{I} = \begin{bmatrix} 1 & 0 & 0 \\ 0 & 1 & 0 \\ 0 & 0 & 1 \end{bmatrix} \end{cases} \tag{8}$$

In real-world applications, obtaining the exact model of a battery is a difficult task. This is because of the presence of model uncertainty, which corresponds to the gap between the known model and the actual/real battery model. Besides, the existence of measurement noise at the output and disturbances that affect the input may not be avoided. The model uncertainty and disturbances are accommodated in the following model.

$$\begin{cases} x(k+1) = (\mathsf{I} + h(\mathsf{A} + \Delta_{\mathsf{A}}(k)))x(k) + h(\mathsf{B} + \Delta_{\mathsf{B}}(k))(u(k) + w(k)) \\ y(k) = \mathsf{C}(x(k)) + (\mathsf{D} + \Delta_{\mathsf{D}}(k))(u(k) + w(k)) + v_1(k) \end{cases} \tag{9}$$

Where Δ_A, Δ_B, and Δ_D represent the gaps between the battery's known and true parameters. $w(k)$ and $v_1(k)$ represent the input disturbance and output measurement noise, respectively.

2.2. Relationship between open circuit voltage and state-of-charge

As described in the previous subsection, the OCV as a function of SOC, $V_{OC}(\xi)$, is generally a nonlinear function. This nonlinear function can be represented using polynomials. Instead, in this paper, we approximate it with a piecewise linear function. We adopt it from Xu *et al.* in [26]. The piecewise linear function of $V_{OC}(\xi)$ is depicted in Figure 2. The curve in Figure 2 is plotted based on the linear function (10), whose parameters are listed in Table 1. In this paper, we assume the known and the real $V_{OC}(\xi)$ function is exactly the same.

$$V_{OC}(\xi) = a_i \cdot \xi + b_i \tag{10}$$

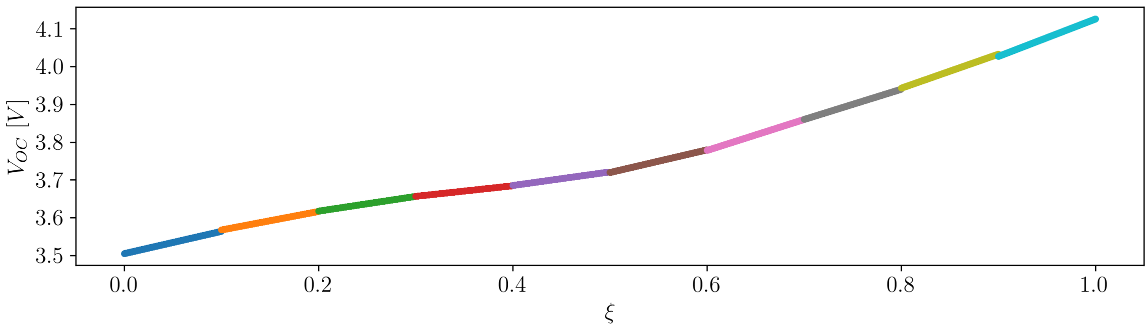

Figure 2. An approximation of the nonlinear relationship between OCV and SOC with a piecewise linear curve

Table 1. Piecewise linear function parameters of $V_{OC}(\xi)$

i	SOC	a_i	b_i	i	SOC	a_i	b_i
1	$0 \leq \xi < 0.1$	0.59	3.5052	6	$0.5 \leq \xi < 0.6$	0.6	3.4199
2	$0.1 \leq \xi < 0.2$	0.49	3.5188	7	$0.6 \leq \xi < 0.7$	0.82	3.2864
3	$0.2 \leq \xi < 0.3$	0.39	3.5397	8	$0.7 \leq \xi < 0.8$	0.8	3.3004
4	$0.3 \leq \xi < 0.4$	0.28	3.5728	9	$0.8 \leq \xi < 0.9$	0.9	3.2232
5	$0.4 \leq \xi < 0.5$	0.36	3.5416	10	$0.9 \leq \xi < 1$	0.99	3.1364

3. MAIN RESULTS AND DISCUSSION

3.1. Proposed observer

Considering (7), A consists of (R_1, C_1) and (R_2, C_2). Suppose we have a sampling period and battery parameters that satisfy the following properties:

$$0 < h\frac{1}{R_1C_1} < 1$$

$$0 < h\frac{1}{R_2C_2} < 1$$

Therefore, we propose the observer as given in (11):

$$\begin{cases} \bar{y}(k) = \mathsf{C}(\bar{x}(k)) + \mathsf{D}\bar{u}(k) \\ \bar{x}(k+1) = (\mathsf{I} + h\mathsf{A})\bar{x}(k) + h\mathsf{B}\bar{u}(k) + h\bar{K}(y(k) - \bar{y}(k)) \end{cases} \tag{11}$$

where

- $\bar{u}(k)$ and $y(k)$ are obtained from sensors, where $\bar{u}(k) = u(k) + v_2(k)$ and a couple $(u(k), y(k))$ is represented in (9).
- $\bar{x}(k) = \begin{bmatrix} \bar{V}_1(k) \\ \bar{V}_2(k) \\ \bar{\xi}(k) \end{bmatrix}$ is the estimated state, where $\bar{\xi}$ is the estimated SOC.
- $\bar{K} = \begin{bmatrix} 0 \\ 0 \\ \kappa \end{bmatrix}$ is the observer gain that satisfies the condition: $\kappa > 0$ such that $0 < h\ \kappa\ \bar{a}_{max} < 1$, where $0 < h < 1$. In addition, $\bar{a}_{max}$ is the maximum coefficient of the linear lines of V_{OC} that refers to value a_i in Table 1.

Figure 3 shows a flowchart of the state-of-charge estimation using our observer. Additionally, it is worth noting that the proposed observer (11) the model with known parameters (7). Besides, to avoid confusion for readers, it is also worth noting that the model in (9) is for numerical simulation purposes. In addition, regarding the properties of (R_1, C_1) and (R_2, C_2) stated above, it is reasonable since the parameters of batteries found in various papers satisfy those properties.

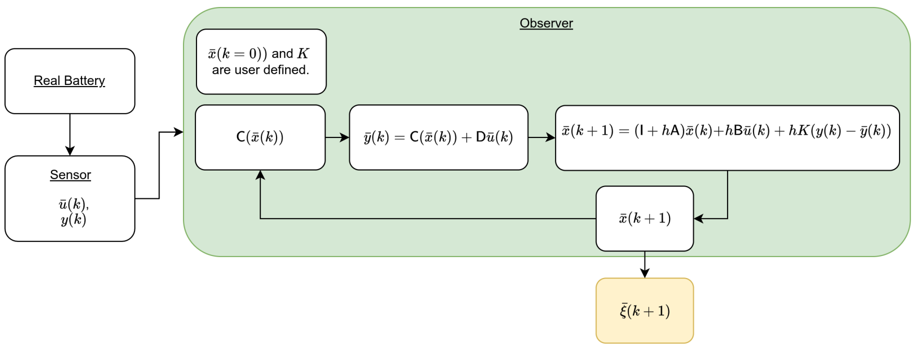

Figure 3. SOC estimation flowchart

3.2. Stability analysis

In this subsection, the stability proof of the proposed observer is elaborated. Now, recall $\bar{V}_{OC}(\xi)$ in (10) and $y(k)$ in (7). Since $V_{OC}(\bar{\xi}(k)) = \bar{a}_i(k)\bar{\xi}(k) + \bar{b}_i(k)$, hence we have the following:

$$\mathsf{C}(\bar{x}(k)) = \bar{H}(x)\bar{x}(k) + \bar{b}_i(k) \tag{12}$$

where

$$\bar{H}(k) = \begin{bmatrix} -1 & -1 & \bar{a}_i(k) \end{bmatrix} \tag{13}$$

In order to reduce the complexity of observer design, we apply the following assumptions:

- For all $k \leq 0$, $\xi(k)$ and $\bar{\xi}(k)$ can be not equal, but both are always on the same piece of a linear line of the $V_{OC} - SOC$ curve. For example, $(\xi, \bar{\xi}) = (0.31, 0.35)$ is on the same piece of a linear line, while $(\xi, \bar{\xi}) = (0.31, 0.55)$ is not on the same piece of a linear line.
- $\Delta_{\mathsf{A}}(k)$, $\Delta_{\mathsf{B}}(k)$, and $\Delta_{\mathsf{D}}(k)$ are all zero. In other words, the real battery parameters are assumed to be known exactly.
- It is assumed that there is no disturbance and noise, i.e., $w(k)$, $v_1(k)$, and $v_2(k)$ are also zero.

Note that these assumptions reflect that the actual battery used for stability analysis is identical to the model battery employed in the observer, namely the model in (7). Let define the estimation error $e_{\bar{x}}(k)$ (14):

$$e_{\bar{x}}(k) = x(k) - \bar{x}(k) = \begin{bmatrix} e_{\bar{x}1}(k) \\ e_{\bar{x}2}(k) \\ e_{\bar{x}3}(k) \end{bmatrix} \tag{14}$$

Regarding the assumption above that ξ and $\bar{\xi}$ are on the same piece of a linear line of the OCV-SOC curve, we have the following.

$$\begin{aligned} e_{\bar{x}}(k+1) &= (\mathsf{I} + h\mathsf{A})e_{\bar{x}} - h\bar{K}\big(y(k) - \bar{y}(k)\big) \\ &= (\mathsf{I} + h\mathsf{A})e_{\bar{x}} - h\bar{K}\bar{H}(k)e_{\bar{x}}(k) \\ &= \big(\mathsf{I} + h\mathsf{A} - h\bar{K}\bar{H}(k)\big)e_{\bar{x}}(k) \end{aligned} \tag{15}$$

Next, motivated by the structure of the nonlinear observer gain in [16], i.e., $\bar{K} = \begin{bmatrix} 0 \\ 0 \\ \kappa \end{bmatrix}$, we consider the following facts:

- The sampling period h is less than $1s$, i.e., $0 < h < 1$.
- Entries of matrix A satisfy $0 < \dfrac{1}{R_1C_1} < 1$ and $0 < \dfrac{1}{R_2C_2} < 1$.
- The coefficient $\bar{a}_i$ satisfies $0 < \bar{a}_i \leq \bar{a}_{max} < 1$.

Now, consider the following Lyapunov function candidate (16) and its forward difference (17).

$$V(k) = e_{\bar{x}1}(k)^T e_{\bar{x}1}(k) > 0,\ \forall e_{\bar{x}1}(k) \neq 0 \tag{16}$$

$$\begin{aligned} \Delta V(k) &= V(k+1) - V_1(k) \\ &= \left(1 - h\frac{1}{R_1C1}\right)^2 e_{\bar{x}1}(k)^2 - e_{\bar{x}1}(k)^2 \\ &= \left(\left(1 - h\frac{1}{R_1C1}\right)^2 - 1\right) e_{\bar{x}1}(k)^2 < 0 \text{ provided that } 0 < h\frac{1}{R_1C_1} < 1 \end{aligned} \tag{17}$$

These facts imply that $e_{\bar{x}1}(k)$ approaches 0 as k approaches infinity. In addition, we can use a similar analysis to prove $e_{\bar{x}2}(k)$ also approaches 0 as k approaches infinity, if it satisfies $0 < h\dfrac{1}{R_2C_2} < 1$.

Now, consider the first Lyapunov function candidate expressed by (18) as follows:

$$\tilde{V}_(k) = e_{\bar{x}3}(k)^T e_{\bar{x}3}(k) > 0,\ \forall e_{\bar{x}3}(k) \neq 0 \tag{18}$$

in addition, its forward difference is given as (19):

$$\begin{aligned} \Delta\tilde{V}(k) &= \tilde{V}(k+1) - \tilde{V}(k) \\ &= \left(e_{\bar{x}3}(k) + h\kappa e_{\bar{x}1}(k) + h\kappa e_{\bar{x}2}(k) - h\kappa\bar{a}_i e_{\bar{x}3}(k)\right)^2 - e_{\bar{x}3}(k)^2 \end{aligned} \tag{19}$$

in the previous description, we know that $e_{\bar{x}1}(k)$ and $e_{\bar{x}2}(k)$ approach 0 as k approaches infinity; hence, we have the following:

$$\begin{aligned} \Delta\tilde{V}(k) &= \left(e_{\bar{x}3}(k) - h\kappa\bar{a}_i e_{\bar{x}3}(k)\right)^2 - e_{\bar{x}3}(k)^2 \\ &= \left((1 - h\kappa\bar{a}_i)^2 - 1\right) e_{\bar{x}3}(k)^2 < 0 \text{ provided that } 0 < h\kappa\bar{a}_i < 1 \end{aligned} \tag{20}$$

to be more generally applicable, the condition becomes $0 < h\kappa\bar{a}_{max} < 1$. It completes the stability analysis.

3.3. Numerical simulation and discussion

Simulations run adopt LIB parameters in [27], for R_S, (R_1, C_1) and $(R_2, C_2$, and in [28], for Q_ξ. All simulations regard that the Coulombic efficiency η is 1 (see (4)). These are shown in Table 2. We utilize Python 3.12.1 for the simulations.

In the first simulation, we show how the situation represents a simplified case as described in the stability analysis above. In this situation, the real and estimated SOC values are on the same piece of a linear line of the V_{OC} curve; the initial conditions of real SOC and estimated SOC values are 0.98 and 0.91, respectively. Besides, the discharge current $u = I$ is set to a constant value, i.e., $-0.49A$. Three values of the observer gain κ are used for comparison of the performance. Figure 4 shows the simulation result. We can notice that the higher observer gain gives a faster estimated SOC approach to the real SOC. Nevertheless, all estimated SOC values tend to provide zero estimation error. Next, it is of interest to see how observers could perform in more practical scenarios.

Table 2. Battery parameters

	Ω		F		Ah
R_1	0.015	C_1	1000	Q_ξ	4.9
R_2	0.0015	C_2	2500		
R_S	0.024				

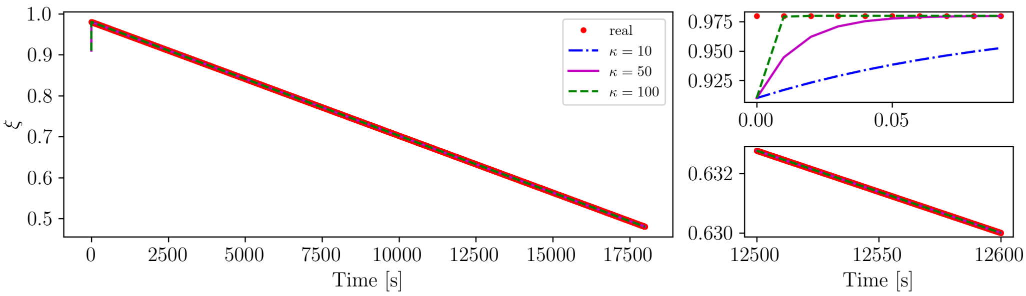

Figure 4. SOC estimation result based on the simplified situation meets the asymptotically stable guarantee

In the second simulation, we set the initial conditions of real SOC and estimated SOC are 0.98 and 0, respectively. Another difference from the previous simulation is that we use the disturbance w and the noise (v_1, v_2), which are the normal random numbers whose maximum amplitude is 0.001. Each normal random number that represents the disturbance and noise is generated uniquely. Figure 5 shows the simulation result. All estimated SOC values tend to reach the real SOC with the same speed as in the first simulation. However, we could identify that the higher observer gain implies a higher distortion amplitude. In addition, at about $2800 - 3000s$ there are jumps (drops and lifts) in the estimated SOC values. It might relate to the nonlinearity of the relationship between OCV and SOC (see Figure 2). However, the important fact is that this indicates there is an error in SOC estimation due to noisy sensor data.

The third simulation includes the uncertainties Δ_A, Δ_B, and Δ_D. These values vary by a maximum 10% of the known parameters (A, B, C). It is implemented by, for example, $\Delta_\mathsf{B} = \mathsf{B} \times 0.1 S_\Delta$, where S_Δ is sine wave with the frequency is $5 \times 10^{-5} Hz$. This simulation result is shown in Figure 6. The result is similar to the previous situation, except that, compared to Figure 5, there is a shift between the real SOC line and the estimated SOC line. It is noticeable at about $2800s$ in the area where the estimated SOC values jump.

Next, we consider using a different profile of the current discharge. It is in the form of pulse width modulation (PWM) whose frequency, duty cycle, and amplitude are $1 \times 10^{-3} Hz$, 10%, and -4 A, respectively. It is called the multiple step test (MST) [29]. The other situations in this simulation are the same as the previous one. The simulation result is depicted in Figure 7. We could notice there are jumps in every occurrence of sudden discharge current. However, the shape is not as similar as the jumps in the previous figures. In this simulation, it appears that there are additional overshoot and undershot properties that usually appear in the step response of a control system. However, it indicates that the observer failed to provide a perfect SOC estimation when a sudden discharged current occurs.

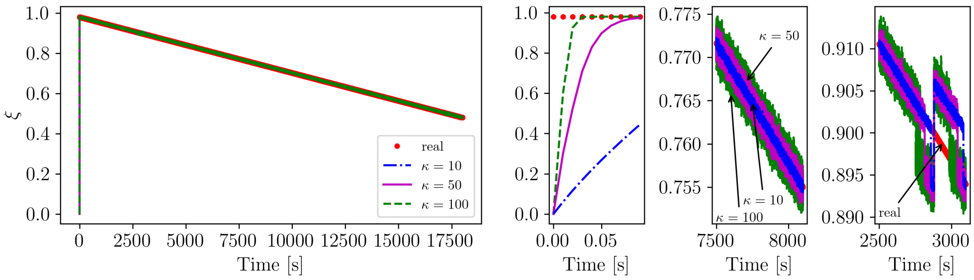

Figure 5. SOC estimation result using the model suffers from disturbance and noise

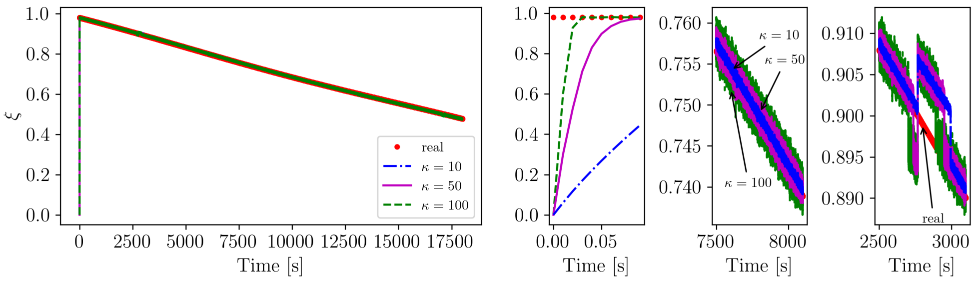

Figure 6. SOC estimation result using the model suffers from disturbance, noise, and model uncertainty

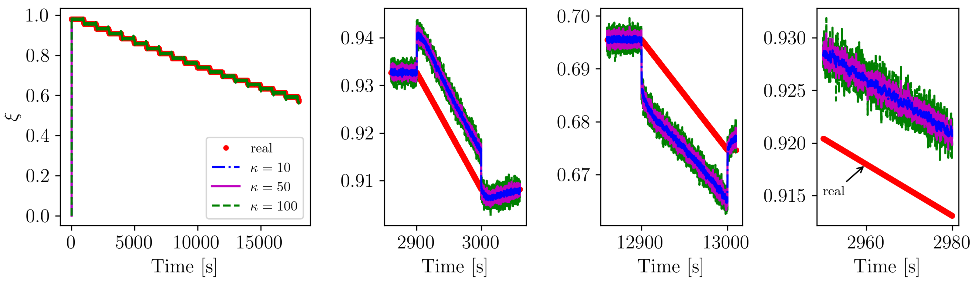

Figure 7. SOC estimation result using the model suffers from disturbance, noise, and uncertainty with a PWM discharge current

4. CONCLUSION

A discrete-time Luenberger observer-based to estimate a Lithium-ion battery's state-of-charge is presented. Some assumptions are used in the stability analysis in order to prevent complexity in the observer design. The observer has an asymptotically stability guarantee. Multiple simulations are conducted to assess the observer's performance. The simulations also consider the situation that corresponds to a realistic situation, such as the unknown initial value of the real battery's state of charge as well as the appearance of disturbance, noise, and model uncertainties. Based on the simulation results, some challenging problems could be considered for further research. One aspect is to utilize a higher observer gain to quickly achieve the actual SOC and a lower observer gain to minimize distortion.

ACKNOWLEDGEMENT

This research is supported by the Rumah Program Purwarupa Sistem Otonom Kendaraan Listrik, Organisasi Riset Elektronika dan Informatika, BRIN, FY 2024. All authors have contributed equally to the work, with the following details: HS = Methodology, Software, Formal analysis, Writing - Original Draft, Writing - Review & Editing; EK = Writing - Review & Editing; JAP = Writing - Review & Editing; SH = Writing - Review & Editing; MWSA = Writing - Review & Editing; OS = Conceptualization, Writing - Review & Editing.

REFERENCES

[1] I. M. Monirul, L. Qiu, R. Ruby, and J. Yu, “Adaptive state of charge estimation for lithium-ion batteries using feedback-based extended Kalman filter,” *IET Control Theory and Applications*, vol. 17, no. 16, pp. 2162–2177, 2023, doi: 10.1049/cth2.12519.

[2] H. Mei, P. Piccardo, A. Cingolani, and R. Spotorno, “Unconventional solid-state electrolytes for lithium-based batteries: Recent advances and challenges,” *Journal of Power Sources*, vol. 553, 2023, doi: 10.1016/j.jpowsour.2022.232257.

[3] N. I. M. Siam, T. Sutikno, and M. J. A. Aziz, “Lithium ferro phosphate battery state of charge estimation using particle filter,” *International Journal of Power Electronics and Drive Systems*, vol. 12, no. 2, pp. 975–985, 2021, doi: 10.11591/ijpeds.v12.i2.pp975-985.

[4] J. C. Burns *et al.*, “Predicting and Extending the Lifetime of Li-Ion Batteries,” *Journal of The Electrochemical Society*, vol. 160, no. 9, pp. A1451–A1456, 2013, doi: 10.1149/2.060309jes.

[5] Q. Ouyang and J. Chen, *Advanced Model-Based Charging Control for Lithium-Ion Batteries.* Singapore: Springer Nature Singapore, 2023.

[6] R. Yin *et al.*, “Risk analysis for marine transport and power applications of lithium ion batteries: A review,” *Process Safety and Environmental Protection*, vol. 181, pp. 266–293, 2024, doi: 10.1016/j.psep.2023.11.015.

[7] J. Zhao, X. Feng, M. K. Tran, M. Fowler, M. Ouyang, and A. F. Burke, “Battery safety: Fault diagnosis from laboratory to real world,” *Journal of Power Sources*, vol. 598, 2024, doi: 10.1016/j.jpowsour.2024.234111.

[8] M. Waseem, M. Ahmad, A. Parveen, and M. Suhaib, “Battery technologies and functionality of battery management system for EVs: Current status, key challenges, and future prospectives,” *Journal of Power Sources*, vol. 580, 2023, doi: 10.1016/j.jpowsour.2023.233349.

[9] L. Lu, X. Han, J. Li, J. Hua, and M. Ouyang, “A review on the key issues for lithium-ion battery management in electric vehicles,” *Journal of Power Sources*, vol. 226, pp. 272–288, 2013, doi: 10.1016/j.jpowsour.2012.10.060.

[10] M. A. Hannan, M. S. H. Lipu, A. Hussain, and A. Mohamed, “A review of lithium-ion battery state of charge estimation and management system in electric vehicle applications: Challenges and recommendations,” *Renewable and Sustainable Energy Reviews*, vol. 78, pp. 834–854, 2017, doi: 10.1016/j.rser.2017.05.001.

[11] T. Duraisamy and D. Kaliyaperumal, “Active cell balancing for electric vehicle battery management system,” *International Journal of Power Electronics and Drive Systems*, vol. 11, no. 2, pp. 571–579, 2020, doi: 10.11591/ijpeds.v11.i2.pp571-579.

[12] L. Zhou *et al.*, “State Estimation Models of Lithium-Ion Batteries for Battery Management System: Status, Challenges, and Future Trends,” *Batteries*, vol. 9, no. 2, 2023, doi: 10.3390/batteries9020131.

[13] W. Li, M. Rentemeister, J. Badeda, D. Jöst, D. Schulte, and D. U. Sauer, “Digital twin for battery systems: Cloud battery management system with online state-of-charge and state-of-health estimation,” *Journal of Energy Storage*, vol. 30, 2020, doi: 10.1016/j.est.2020.101557.

[14] Z. Li, J. Huang, B. Y. Liaw, and J. Zhang, “On state-of-charge determination for lithium-ion batteries,” *Journal of Power Sources*, vol. 348, pp. 281–301, Apr. 2017, doi: 10.1016/j.jpowsour.2017.03.001.

[15] S. Mukherjee and K. Chowdhury, “State of charge estimation techniques for battery management system used in electric vehicles: a review,” *Energy Systems*, 2023, doi: 10.1007/s12667-023-00631-x.

[16] A. Hasan, M. Skriver, and T. A. Johansen, “Exogenous Kalman Filter for State-of-Charge Estimation in Lithium-Ion Batteries,” in *IEEE Conference on Control Technology and Applications, CCTA*, 2018, pp. 1403–1408, doi: 10.1109/CCTA.2018.8511577.

[17] G. L. Plett., *Battery Management Systems, Volume II: Equivalent-Circuit Methods.* 2015.

[18] A. Seaman, T. S. Dao, and J. McPhee, “A survey of mathematics-based equivalent-circuit and electrochemical battery models for hybrid and electric vehicle simulation,” *Journal of Power Sources*, vol. 256, pp. 410–423, 2014, doi: 10.1016/j.jpowsour.2014.01.057.

[19] S. Nejad, D. T. Gladwin, and D. A. Stone, “A systematic review of lumped-parameter equivalent circuit models for real-time estimation of lithium-ion battery states,” *Journal of Power Sources*, vol. 316, pp. 183–196, 2016, doi: 10.1016/j.jpowsour.2016.03.042.

[20] J. Meng *et al.*, “An Overview and Comparison of Online Implementable SOC Estimation Methods for Lithium-Ion Battery,” *IEEE Transactions on Industry Applications*, vol. 54, no. 2, pp. 1583–1591, 2018, doi: 10.1109/TIA.2017.2775179.

[21] Y. Wang *et al.*, “A comprehensive review of battery modeling and state estimation approaches for advanced battery management systems,” *Renewable and Sustainable Energy Reviews*, vol. 131, 2020, doi: 10.1016/j.rser.2020.110015.

[22] N. Ghaeminezhad, Q. Ouyang, J. Wei, Y. Xue, and Z. Wang, “Review on state of charge estimation techniques of lithium-ion batteries: A control-oriented approach,” *Journal of Energy Storage*, vol. 72, 2023, doi: 10.1016/j.est.2023.108707.

[23] D. Luenberger, “An introduction to observers,” *IEEE Transactions on Automatic Control*, vol. 16, no. 6, pp. 596–602, Dec. 1971, doi: 10.1109/TAC.1971.1099826.

[24] H. Septanto, E. Kurniawan, J. A. Prakosa, S. Hafiz, M. W. Surya Atman, and O. Sudjana, “Asymptotically Stable Discrete-Time Observer for State-of-Charge Estimation,” in *International Conference on Advanced Mechatronics, Intelligent Manufacture and Industrial Automation (ICAMIMIA)*, Nov. 2023, pp. 183–188, doi: 10.1109/ICAMIMIA60881.2023.10427837.

[25] M. Juston, N. Damay, and C. Forgez, “Extracting the diffusion resistance and dynamic of a battery using pulse tests,” *Journal of Energy Storage*, vol. 57, 2023, doi: 10.1016/j.est.2022.106199.

[26] J. Xu, C. C. Mi, B. Cao, J. Deng, Z. Chen, and S. Li, “The state of charge estimation of lithium-ion batteries based on a proportional-integral observer,” *IEEE Transactions on Vehicular Technology*, vol. 63, no. 4, pp. 1614–1621, 2014, doi: 10.1109/TVT.2013.2287375.

[27] M. Al-Gabalawy, N. S. Hosny, J. A. Dawson, and A. I. Omar, “State of charge estimation of a Li-ion battery based on extended Kalman filtering and sensor bias,” *International Journal of Energy Research*, vol. 45, no. 5, pp. 6708–6726, 2021, doi: 10.1002/er.6265.

[28] J. Yun, Y. Choi, J. Lee, S. Choi, and C. Shin, “State-of-Charge Estimation Method for Lithium-Ion Batteries Using Extended Kalman Filter With Adaptive Battery Parameters,” *IEEE Access*, vol. 11, pp. 90901–90915, 2023, doi: 10.1109/ACCESS.2023.3305950.

[29] M. Ceraolo, G. Lutzemberger, D. Poli, and C. Scarpelli, “Luenberger based State Of Charge evaluation and experimental validation with lithium cells,” *Journal of Energy Storage*, vol. 30, 2020, doi: 10.1016/j.est.2020.101534.

BIOGRAPHIES OF AUTHORS

Harry Septanto is a researcher at the National Research and Innovation Agency (BRIN), Indonesia. He received his B.Eng., M.Eng., and Ph.D. degrees from Institut Teknologi Bandung in Engineering Physics, Electrical Engineering, and Electrical Engineering & Informatics, in 2002, 2010, and 2015, respectively. He has been a *Peneliti Ahli Utama* in BRIN, Indonesia, since 2024. He is currently a Section Editor of the Jurnal Elektronika dan Telekomunikasi (JET). His research interests include control and signal & systems. He can be contacted at email: harr004@brin.go.id.

Edi Kurniawan is currently with the Control and Precision Measurement Research Group, Research Centre for Photonics, National Research and Innovation Agency (BRIN). He received B.Eng. degree (cumlaude) from Gadjah Mada University, Indonesia, in 2003, and M.Eng. degree from the University of Adelaide, Australia, in 2009, both in electrical and electronics engineering. He completed his Ph.D. in 2013 from Swinburne University of Technology, Australia, in the field of control system. His research interests include learning control, robust control, adaptive control, speech recognition, signal and image processing, and deep learning. He can be contacted at email: edik004@brin.go.id.

Jalu Ahmad Prakosa is a senior researcher at the Precision Control and Measurement Research Group (KPP), Photonics Research Center, Nanotechnology and Materials Research Organization (ORNM), National Research and Innovation Agency (BRIN). He received B.Sc. in Electronics and Instrumentation from Gadjah Mada University(UGM), Indonesia, in Automation and Mechatronics from Saint-Petersburg Electrotechnical University ETU "LETI", Russia. Currently, he is working on a Ph.D. in Mathematics at Universiti Teknologi Malaysia(UTM), Malaysia. His research areas include physics instrumentation, measurement, mathematical modeling, control systems, artificial intelligence, internet of things (IoT), and optimization. He can be contacted at email: jalu002@brin.go.id.

Samsul Hafiz is a researcher at the National Research and Innovation Agency (BRIN). Currently, he is working on a Ph.D. on the topic of battery cell balancing at Universitas Indonesia, Indonesia. His research areas include energy, electronics, and instrumentation. He can be contacted at email: sams013@brin.go.id.

Made Widhi Surya Atman received the B.Eng. and M.Sc. degrees in electrical engineering from Institut Teknologi Bandung, Indonesia, in 2011 and 2014, respectively, and the M.Eng. degree in mechanical and control engineering and the D.Eng. degree in systems and control engineering from the Tokyo Institute of Technology, in 2017 and 2020, respectively. Since 2020, he has been a Postdoctoral Research Fellow of automation technology and mechanical engineering with Tampere University. His research interests include human-swarm interaction, passivity-based control, and distributed control of networked systems. He can be contacted at email: widhi.atman@tuni.fi.

Oetomo Sudjana received the B.Eng. and M.Sc. degrees in electrical engineering from Universitas Udayana, Indonesia, and Institut Teknologi Bandung, Indonesia, respectively. He is a Technical Lead at PT Teknologi Rakyat Indonesia. He can be contacted at email: oektomo@gmail.com.